Eva Oberacker*, Andre Kuehne, Jacek Nadobny, Sebastian Zschaeck, Mirko Weihrauch, Helmar Waiczies, Pirus Ghadjar, Peter Wust, Thoralf Niendorf and Lukas Winter

# Radiofrequency applicator concepts for simultaneous MR imaging and hyperthermia treatment of glioblastoma multiforme

## A 298 MHz (7.0 Tesla) thermal magnetic resonance simulation study

**Abstract:** Glioblastoma multiforme is the most frequent and most aggressive malignant brain tumor with de facto no long term curation by the use of current multimodal therapeutic approaches. The efficacy of brachytherapy and enhancing interstitial hyperthermia has been demonstrated. RF heating at ultrahigh fields ($B_0$=7.0T, f=298MHz) has the potential of delivering sufficiently large thermal dosage for hyperthermia of relatively large tumor areas. This work focuses on electromagnetic field (EMF) simulations and provides realistic applicator designs tailored for simultaneous RF heating and MRI. Our simulations took advantage of target volumes derived from patient data, and our preliminary results suggest that RF power can be focused to both a small tumor area and a large clinical target volume.

**Keywords:** Thermal Magnetic Resonance, RF heating, hyperthermia, glioblastoma multiforme, RF applicator.

──────
**\*Corresponding author: Eva Oberacker:** Berlin Ultrahigh Field Facility (B.U.F.F.), Max Delbrück Centrum for Molecular Medicine in the Helmholtz Association, Robert-Rössle-Str. 10, 13125 Berlin, Germany, e-mail: eva.oberacker@mdc-berlin.de
**Andre Kuehne, Helmar Waiczies, Thoralf Niendorf:** MRI.TOOLS GmbH, Berlin, Germany
**Jacek Nadobny, Sebastian Zschaeck, Mirko Weihrauch, Pirus Ghadjar, Peter Wust:** Clinic for Radiation Oncology, Charité Universitätsmedizin, Berlin, Germany
**Thoralf Niendorf, Lukas Winter:** Berlin Ultrahigh Field Facility (B.U.F.F.), Max Delbrück Centrum for Molecular Medicine in the Helmholtz Association, Berlin, Germany
**Thoralf Niendorf:** Experimental and Clinical Research Center (ECRC), a joint cooperation between the Charité Medical Faculty and the Max Delbrück Center for Molecular Medicine in the Helmholtz Association, Berlin, Germany

# 1 Introduction

Glioblastoma multiforme is the most frequent and aggressive malignant braintumor with no long term curation by the use of current multimodal therapeutic approaches [1]. A prospective randomized trial showed the principal effectiveness of brachytherapy and enhancing interstitial hyperthermia, prolonging median survival [2]. The invasiveness of this approach is a major road blocker for wider clinical application, thus the need for non-invasive thermal therapy solutions is obvious. Simultaneous RF-heating and MR imaging at ultrahigh fields ($B_0$=7.0T, f=298MHz) [3-7] has the potential of delivering and managing sufficiently large thermal dosage for hyperthermia of relatively large tumor areas. En route to a potential RF-induced hyperthermia treatment of glioblastoma in the human brain, this work focuses on electromagnetic field (EMF) simulations and provides realistic RF applicator designs tailored for simultaneous RF-heating and MRI.

# 2 Methods

EMF simulations [8] were performed in for two voxel models of the human head:
- Voxel model "Duke" [9] was upgraded with a sphere (d=4cm, $\sigma_{Tumor}$=1.15S/m, $\varepsilon_{Tumor}$=66.5 [10], **Figure 1**a).
- A real clinical computed tomography (CT) dataset of a patient with glioblastoma multiforme was segmented into 18 contours and assigned respective EM material properties of tissue [11] (**Figure 1**b). The model differentiates two regions in the brain: the tumor (dark yellow) and the clinical target volume (CTV) which is subject to radiotherapy planning.
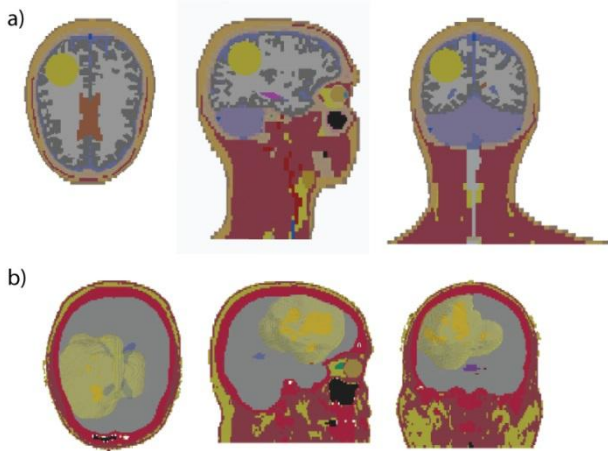
**Figure 1:** a) Axial, sagittal and coronal view of the human voxel model "Duke" at the central slice of the superimposed spherical tumor (d=4cm). b) Axial, sagittal and coronal view of the voxel model based on a patient's CT dataset showing the tumor (dark yellow) and the much bigger clinical target volume (CTV) in light yellow.

Three RF antenna arrays were modeled, each comprising bowtie electric dipole antennae in a circular arrangement. These building blocks demonstrated good RF heating and MR imaging performance at f=298MHz [3,12]. Design1 consists of eight antennae ((35x70x150) mm³ each) positioned symmetrically (diameter = 24cm) around the human head (**Figure 2**a,b) with $D_2O$ ($\varepsilon \approx 80$) as high permittivity medium for wavelength shortening and antenna size reduction [13]. Design2 constitutes a 16-channel array ((40x40x80) mm³ each; **Figure 2**c,d). A higher permittivity dielectric ($\varepsilon \approx 200$) allowed further antenna size reduction and can be realized by mixing high permittivity $BaTiO_3$ powder with $D_2O$. For design3, 16 antennae ((40x40x80)mm³, $\varepsilon \approx 200$) were positioned interleaved along the z-direction (**Figure 2**e,f). Copper sheets were used to decrease next neighbor coupling (**Figure 2**d,f).
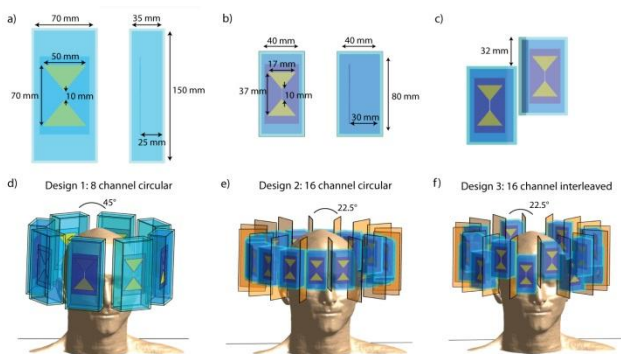


**Figure 2:** a) Schematic of a bowtie dipole building block filled with $D_2O$; b) Schematic of bowtie dipole building block filled with $BaTiO_3$; c) Disalignment of the elements in the interleaved array. d) Design1: 8 element ring array with $D_2O$ dipoles; e) Design2:16 element ring array with $BaTiO_3$ dipoles; f) Design3:16 element interleaved array with $BaTiO_3$ dipoles.
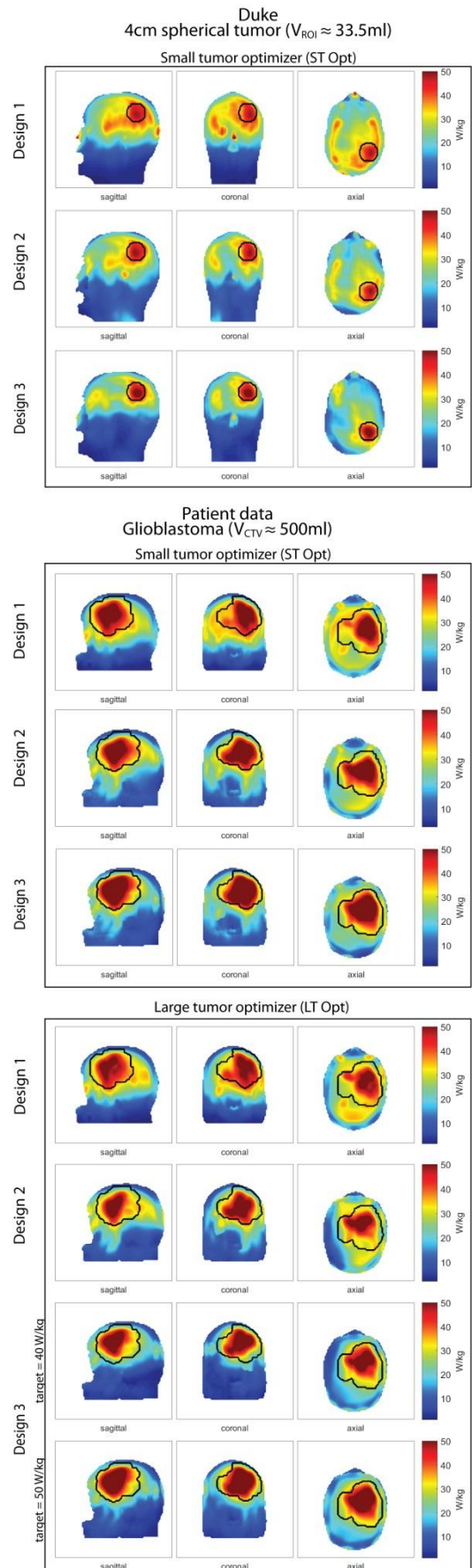


**Figure 3:** Maximum intensity projections of $SAR_{10g}$ distributions

For the proposed RF-applicator designs and tumor models, the E-fields of the transmit elements were combined [14-18] using an optimization algorithm [19] for the specific absorption rate (SAR)-distributions. Different constraints namely the maximum $SAR_{10g}$ in healthy tissue and the maximum total power delivered to the head were set. To cover a broad range of tumor sizes, shapes and locations in patients, two optimizers were implemented: (i) aiming for a maximum RF power deposition in the target region and (ii) simultaneously targeting a uniform distribution of the RF power while sparing surrounding healthy tissue (consideration of "organs at risk"). The uniformity of the power distribution can be traded for higher peak $SAR_{10g}$ values in the target region by increasing the constraint "target".

# 3 Results

**Figure 3:** The maximum intensity projections show the $SAR_{10g}$ distribution in the ROI (top) and the CTV (middle and bottom) for all applicator designs. For the CTV, the small tumor optimizer (ST Opt) and and large tumor optimizer (LT Opt) are compared. For LT Opt of design3, the results for two target values are displayed. The $SAR_{10g}$ limit is set to 40W/kg for the therapeutical approach [20]. Design 3 enables tumor heating with lower $SAR_{10g}$ values in the healthy tissue, sparing the surrounding organs at risk (OAR) for both tumor models. ST Opt reaches higher peak $SAR_{10g}$ values in the CTV while exposing the OAR to a higher power deposition. The readout for maximum tumor SAR10g, total delivered power to the target region and total head power are summarized in **Table 1**.

**Figure 4:** Quantification of the power distribution for all designs and tumor models is done for the total power delivered to the ROI/CTV (top), the fraction of the ROI/CTV with $SAR_{10g}$ levels above the $SAR_{10g}$(OAR) limit (middle) and the uniformity of the power distribution (bottom). For all cases, the optimization runs into saturation for a certain allowed total head power $P_{Head}$ (icons change from bold to empty). Design 3 reaches said saturation with lower $P_{Head}$, i.e. sparing the OAR, but nevertheless outperforms the other designs in RF power delivery. This indicates the importance of introducing the longitudinal dimension in the array for better hotspot steering. A small trade-off has to be accepted in terms of uniformity of the power distribution.

Furtheron, we found that ST Opt obtains superior RF power delivery in the large tumor while the setback in uniformity is only minor.

**Table 1:** Optimization results for all models, designs and optimizers

| Model | Design | | $SAR_{max}$(Tumor) [W/kg] | $P_{Tumor}$ [W] | $P_{Head}$ [W] |
|---|---|---|---|---|---|
| **Duke + ST Opt** | 1 | | 49.14 | 1.61 | 78.08 |
| | 2 | | 49.79 | 1.61 | 81.18 |
| | 3 | | 53.32 | 1.71 | 61.58 |
| **CTV + ST Opt** | 1 | | 62.05 | 15.95 | 94.96 |
| | 2 | | 70.35 | 16.88 | 94.26 |
| | 3 | | 92.00 | 19.04 | 86.57 |
| **CTV + LT Opt** | 1 | | 57.13 | 15.46 | 89.08 |
| | 2 | | 60.51 | 15.32 | 84.66 |
| | 3 | target = 40 | 64.66 | 15.29 | 65.46 |
| | | target = 50 | 83.66 | 17.57 | 74.69 |

# 4 Discussion and conclusion

Our preliminary results suggest that RF power can be focused to both a small tumor area (V≈33ml) and a large clinical target volume (V≈500ml) based on segmented patient data used in this work. A higher number of transmit RF channels arranged in an interleaved manner improves hyperthermia performance. To take our work to the next level the simulation setup will be extended to temperature optimizations using temperature matrices [21] in order to calculate thermal dose (CEM43°C) distributions [22].
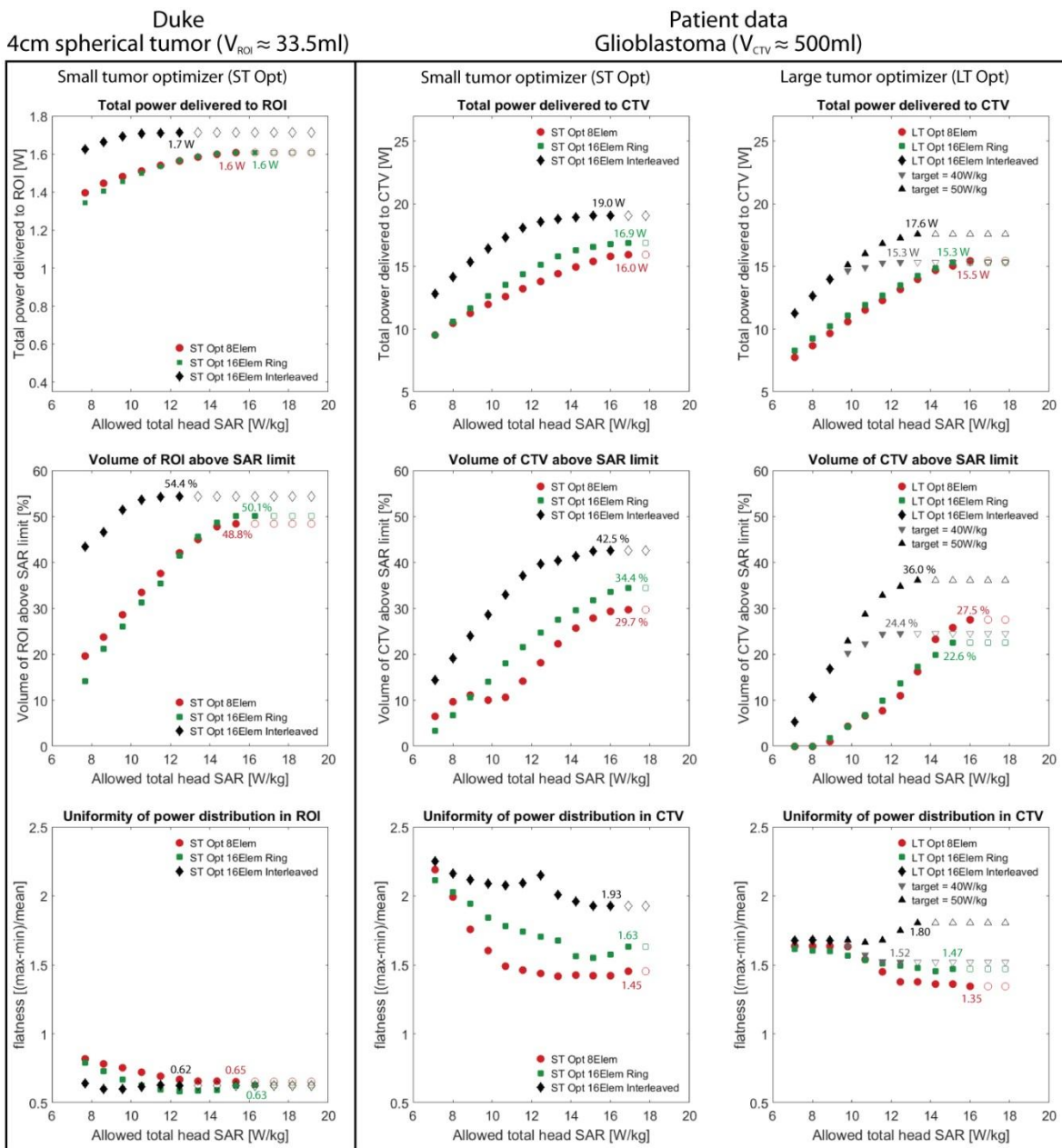
**Figure 4:** Quantitative evaluation of optimizer performance for Duke with the 4cm tumor (left) and the patient voxel model (middle and right) comparing the total delivered power (top), the fraction of the target region with a SAR higher than the given limit for the OAR (40W/kg) and the non-uniformity of the power distribution (bottom).

# References

[1] World Cancer Report 2014, World Health Organisation;

[2] Sneed, PK, Stauffer PR, et al., Survival benefit of hyperthermia in a prospective randomized trial of brachytherapy boost±hyperthermia for glioblastoma multiforme. Int J of Radiation Oncology* Biology* Physics, 1998:40: 287-295.

[3] Winter L, Özerdem C, Hoffmann W, et al., Design and Evaluation of a Hybrid Radiofrequency Applicator for Magnetic Resonance Imaging and RF Induced Hyperthermia: Electromagnetic Field Simulations up to 14.0 Tesla and Proof-of-Concept at 7.0 Tesla. PLoS One, 2013:8:e61661.

[4] Winter L, Oezerdem C, Hoffmann W, et al., Thermal magnetic resonance: physics considerations and electromagnetic field simulations up to 23.5 Tesla (1GHz). Radiation Oncology, 2015:10:1.

[5] Guerin B, Villena JF, Polimeridis AG, et al., Ultimate hyperthermia: Computation of the best achievable radio-frequency hyperthermia treatments in non-uniform body models, Proceedings of the 24th ISMRM, 2016.

[6] Pendse M and Rutt B, An algorithm for maximum-SAR Targeted RF Hyperthermia, Proceeding of 23rd ISMRM, 2015.

[7] Ertürk MA, Hegde SS and Bottomley PA, Radiofrequency Ablation, MR Thermometry, and High-Spatial-Resolution MR Parametric Imaging with a Single, Minimally Invasive Device. Radiology, 2016:151447.

[8] Sim4LifeV2.0, ZMT, Zurich, Switzerland;

[9] IT'IS foundation, Zurich, Switzerland;

[10] Restivo MC, van den Berg CA, van Lier AL, et al., Local specific absorption rate in brain tumors at 7 tesla. Magnetic Resonance in Medicine, 2016:75:381-9.

[11] Christ A, Kainz W, Hahn EG, et al., The Virtual Family -- development of surface-based anatomical models of two adults and two children for dosimetric simulations. Physics in medicine and biology, 2009:55: N23.

[12] Oezerdem C, Winter L, Graessl A, et al., 16-Channel Bow Tie Antenna Transceiver Array for Cardiac Mr at 7.0 Tesla. Magnetic Resonance in Medicine, 2016:75: 2553-2565.

[13] Raaijmakers AJ, Ipek O, Klomp DW, et al., Design of a radiative surface coil array element at 7 T: the single-side adapted dipole antenna. Magn Reson Med, 2011: 66: 1488-97.

[14] Volken W, Frei D, Manser P, et al., An integral conservative gridding--algorithm using Hermitian curve interpolation. Phys. Med. Biol. 2008;53:6245 -63. doi: 10.1088/0031-9155/53/21/023.

[15] The MathWorks Inc., Natick, USA;

[16] Kuehne A, Seifert F, Ittermann B. GPU-accelerated SAR computation with arbitrary averaging shapes. Proceedings of the ISMRM. Melbourne, Australia; 2012. p. 4260.

[17] Eichfelder G and Gebhardt M, Local specific absorption rate control for parallel transmission by virtual observation points. Magnetic Resonance in Medicine, 2011. 66: 1468-76.

[18] Luo ZQ, Ma WK, So AMC, Ye Y and Zhang S, Semidefinite relaxation of quadratic optimization problems. IEEE Signal Processing Magazine, 2010. 27: 20.

[19] Grant MC, Boyd SP and Ye Y, CVX: Matlab software for disciplined convex programming (web page and software). Available at http://cvxr.com/cvx.

[20] Wust P. (2016). Thermotherapy in oncology, UNI-MED Verlag;

[21] Boulant N, Wu X, Adriany G, Schmitter S, Uɫurbil K, Van De Moortele PF. Direct control of the temperature rise in parallel transmission by means of temperature virtual observation points: Simulations at 10.5 tesla. Magn. Reson. Med. 2016;75:249 -256. doi: 10.1002/mrm.25637.

[22] van Rhoon GC, Samaras T, Yarmolenko PS, et al., CEM43° C thermal dose thresholds: a potential guide for magnetic resonance radiofrequency exposure levels? Eur Radiol, 2013. 23: 2215-27.